AIP Journal of Applied Physics

Design and modeling of InP-based InGaAs/GaAsSb type-II “W” type quantum wells for mid-Infrared laser applications

C. H. Pan and C. P. Lee

Citation: Journal of Applied Physics **113**, 043112 (2013); doi: 10.1063/1.4789634
View online: http://dx.doi.org/10.1063/1.4789634
View Table of Contents: http://scitation.aip.org/content/aip/journal/jap/113/4?ver=pdfcov
Published by the AIP Publishing

Articles you may be interested in

Room-temperature mid-infrared “M”-type GaAsSb/InGaAs quantum well lasers on InP substrate
J. Appl. Phys. **115**, 063104 (2014); 10.1063/1.4865170

InP-based dilute-nitride mid-infrared type-II “W” quantum-well lasers
J. Appl. Phys. **96**, 4653 (2004); 10.1063/1.1794898

Investigation of the optical properties of InGaAsN GaAs GaAsP multiple-quantum-well laser with 8-band and 10-band k · p model
J. Appl. Phys. **96**, 4663 (2004); 10.1063/1.1792804

Effects of tensile strain in barrier on optical gain spectra of GaInNAs/GaAsN quantum wells
J. Appl. Phys. **93**, 5836 (2003); 10.1063/1.1566469

Theoretical investigation of mid-infrared interband cascade lasers based on type II quantum wells
J. Appl. Phys. **84**, 5357 (1998); 10.1063/1.368789

Re-register for Table of Content Alerts

Create a profile.
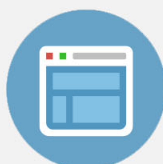
Sign up today!
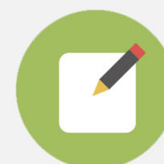

[This article is copyrighted as indicated in the article. Reuse of AIP content is subject to the terms at: http://scitation.aip.org/termsconditions. Downloaded to] IP: 140.113.38.11 On: Thu, 01 May 2014 01:05:00

Design and modeling of InP-based InGaAs/GaAsSb type-II "W" type quantum wells for mid-Infrared laser applications

C. H. Pan and C. P. Lee
Department of Electronics Engineering, National Chiao Tung University, Hsinchu 300, Taiwan

(Received 22 September 2012; accepted 11 January 2013; published online 29 January 2013)

We have theoretically studied the InP based InGaAs/GaAsSb /InAlAs type-II "W" quantum wells (QWs) using the eight band *k.p* theory. The trade-off between the emission wavelength and the magnitude of the transition matrix element was investigated with various structural parameters of the "W" QWs. For the same emission wavelength, the devices with thinner InGaAs/GaAsSb layers and a higher Sb content in GaAsSb could provide higher transition strength. The gain spectra and their peak values at various carrier densities were calculated. We have also found that a more balanced electron and hole masses in the type-II "W" QWs can benefit the material gain. In our designed cases, we have seen that the reduced hole effective mass due to a higher Sb content can partially compensate the gain loss caused by the reduced transition matrix element. Based on the optimized design, a material gain above $10^3\,cm^{-1}$ is readily achievable for a single properly designed "W" quantum well. © *2013 American Institute of Physics*. [http://dx.doi.org/10.1063/1.4789634]

I. INTRODUCTION

The optoelectronic devices based on type-II InGaAs/GaAsSb heterostructures on InP substrates have attracted a lot of interest recently.[1–4] The type-II staggered band alignment offers a good way to extend the devices' operating wavelength into the mid infrared (mid-IR) region, which is important for applications such as molecular absorption spectroscopy, medical care, and free-space optical communication in atmospheric transparency windows.[5,6] Traditionally, semiconductor mid-IR lasers are made on unpopular and expensive GaSb and InAs substrates. It is, however, much more desirable to use a substrate like InP, which is cheaper, has a better thermal conductivity, and a more mature material processing technology. But because of the constraint of lattice mismatch, it is difficult to fabricate such lasers to work at long wavelengths if one uses conventional type I heterostructures. However, when using type II heterostructures, one is able to alleviate some of the constraint by choosing materials that have closer lattice constant to InP and achieve longer wavelength emission via electron-hole recombination across the heterojunction. Although spatial indirect recombination of type-II heterostructure enables an optical transition with energy smaller than the bandgaps of constituent materials, it has a problem of small optical gain due to diminished electron-hole wavefunction overlap. To avoid such problem, the "W" type structure was proposed by adding barrier layers to confine carriers and thereby enhancing the wave function overlap and the optical momentum matrix elements.[7–10] Both electrically injected and optically pumped room temperature InP-based mid-IR lasers using "W" quantum wells (QWs) have been demonstrated with wavelength up to $\sim$2.5 μm.[3,4] Room temperature photoluminescence has shown recently that such structure is capable of light emission with wavelengths beyond 3 μm.[11]

To aid the design of such complex structure, we have performed a comprehensive theoretical study of W type QWs on InP substrates using the eight band *k.p* theory. Here, we are not just limited to the matrix element calculations, as have been done previously,[9,11] which only gives information on the relative emission strength. We have also calculated the material gain spectra, which relate more closely to real laser operations.

II. BAND ALIGNMENT OF THE "W" QW STRUCTURE

A typical band alignment of the "W" type QW together with the electron and hole ground state wavefunctions is shown in Fig. 1. For layers lattice matched to InP, $In_{0.53}Ga_{0.47}As$, and $In_{0.52}Al_{0.48}As$ are used for the wells and the barriers for electrons. The middle layer is the $GaAs_{1-x}Sb_x$ well for the hole confinement. While x = 0.49 is the lattice match condition for $GaAs_{1-x}Sb_x$, we assumed that it can be grown pseudomorphically and used the Sb content as a varying parameter for device optimization. The structure gains the name from the "W"-like shape of conduction band profile. Because of the type-II band alignment, holes are confined inside the valence band (VB) of GaAsSb QW, forming heavy hole (HH) and light hole (LH) sub-bands, and

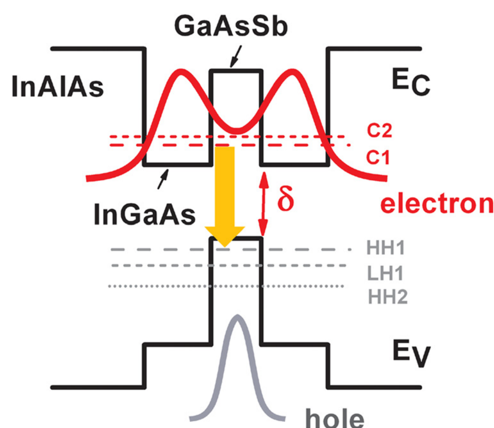

FIG. 1. The band alignment for a typical "W" type QW along with the ground state electron and hole wavefunctions.

 © 2013 American Institute of Physics

[This article is copyrighted as indicated in the article. Reuse of AIP content is subject to the terms at: http://scitation.aip.org/termsconditions. Downloaded to] IP: 140.113.38.11 On: Thu, 01 May 2014 01:05:00

electrons are confined in the two coupled InGaAs QWs, which have the split symmetric (C1) and the anti-symmetric (C2) states. The fundamental C1-HH1 optical transition has a smaller effective band gap energy not limited by the bandgaps of the constituent layers and therefore gives a longer emission wavelength. The barrier layers provide quantum confinement for the electrons and increase the electron-hole wavefunction overlap, which leads to enhanced momentum matrix elements for optical device operation. Two dimensional densities of states for both carries are preserved in the "W" structure.

It is known that the conduction band (CB) edge of InGaAs lowers as the indium mole fraction increases, while the VB edge of GaAsSb goes up with the antimony mole fraction. Either way leads to a decreased energy difference (denoted as δ in Fig. 1) between the CB edge of InGaAs and the VB edge of GaAsSb and hence helps to extend the emission wavelength. Fig. 2 shows the relative position of the band edges of the materials used in the "W" QW. The Sb mole fraction in $GaAs_{1-x}Sb_x$ is varied from 0 to 1. The top horizontal axis indicates the biaxial strain in the GaAsSb layer, which is assumed to be pseudomorphically grown with the same in-plane lattice constant as InP. The band lineup for the lattice-matched case ($GaAs_{0.51}Sb_{0.49}$) is made consistent with the experimentally determined value reported in the literature.[12] The amount of shift in the band edge of pseudomorphic GaAsSb layer is calculated based on "model solid" theory. The deformation potential values are taken from Ref. 13. The energy difference (δ) shrinks as the Sb fraction, x, increases. It is only about 0.25 eV when x is 0.8. This energy corresponds to a very respectable 4.96 μm mid-IR light emission (without adding the electron and hole quantized energies). It should also be mentioned that as the Sb content in GaAsSb increases above the lattice matched condition, the compressive strain in the layer also causes the hole effective mass in the well to decrease. This creates a more favorable electron/hole effective mass balance, which can lead to a reduction in the lasing transparency carrier density.

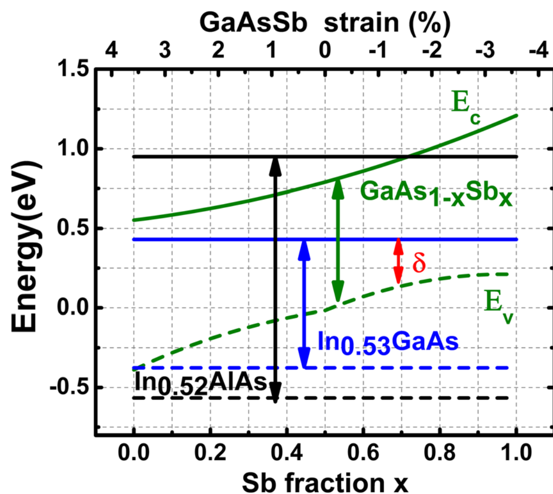

FIG. 2. Band edge energy positions (E_c and E_v) of $In_{0.53}Ga_{0.47}As$ and $In_{0.52}Ga_{0.48}As$, which are lattice matched to InP, and the $GaAs_{1-x}Sb_x$ pseudomorphic layer with Sb fraction varied from 0 to 1. The biaxial strain is indicated on the top horizon axis.

III. THE CALCULATION RESULTS AND DISCUSSION

In this work, the influences of the three most important structural parameters of the W shape QW on the emission wavelength, optical transition, matrix element, and the material gain were investigated. They were (1) the thickness of the $In_{0.53}Ga_{0.47}As$ layer, which was varied from 2 nm to 7 nm, (2) the GaAsSb layer thickness, varied from 2 nm to 5 nm, and (3) the Sb mole fraction of GaAsSb, which was changed from 0.5 to 0.9. Other parameters used (at 300 K) in the calculations were taken from Ref. 13 and listed in Table I. We did not vary the indium content in the InGaAs electron confining layer. Although a higher In content could extend the emission wavelength, the reduced bandgap in this layer would result in a lower electron effective mass. This would create a more unbalanced electron/hole effective masses in our system and hurt the transparency condition and the material gain. So for the purpose of extending the emission wavelength, we chose, in stead, to vary the Sb content in the hole quantum well, where a higher Sb content would reduced the hole effective mass because of a higher compressive strain. This results a more balanced electron/hole effective mass and creates a more favorable situation for the transparency condition and the material gain. The basic framework of the eight band $k.p$ method and the material gain calculation followed those described in Refs. 14 and 15. The layers were assumed to be grown on the (001) surface. The material gain calculation incorporated the Lorenzian line broadening function and can be expressed by the form

$$g(\hbar\omega) = \frac{\pi e^2}{n_r c \varepsilon_0 m_0^2 \omega} \frac{1}{L_z} \sum_{\eta,\sigma} \sum_{n,m} \int |\hat{e} \cdot P_{nm}^{\eta\sigma}|^2 \times \frac{\Gamma/(2\pi)}{[E_{hm}^{en}(k_t) - \hbar\omega]^2 + (\Gamma/2)^2} \times (f^{\eta n} - f^{\sigma m}) \frac{k_t dk_t}{2\pi},$$

with the following parameter notations:n_r :refraction index; m_0 : free electron mass; ε_0 : permittivity in free space; c :light velocity; L_z : *QW thickness*; $|\hat{e} \cdot P_{nm}^{\eta\sigma}|^2$: squared momentum matrix element, $\hat{e}$ is the electric field polarization vector;

TABLE I. The parameters of the constituent materials in the "W" QW used for the $k.p$ calculations.

T = 300 K	$In_{0.52}Al_{0.48}As$	$In_{0.53}Ga_{0.47}As$	$GaAs_xSb_{1-x}$
E_g (eV)	1.45	0.74	$0.812 - 0.723x + 1.43x^2$
E_v (eV)	0	0.19	$0.678 + 0.29x - 1.06x^2$
E_c (eV)	1.45	0.93	$1.49 - 0.433x + 0.37x^2$
Δ (eV)	0.30	0.33	$0.76 - 1.019x + 0.6x^2$
$g_{1(Luttinger)}$	12.20	13.88	$14.5 - 7.52x$
$g_{2(Luttinger)}$	4.81	5.47	$3 - 0.94x$
$g_{3(Luttinger)}$	5.47	6.25	$6 - 307x$
E_p (eV)	21.31	24.93	$27 + 1.8x$
a (Å)	5.87	5.87	$6.096 - 0.443x$
C11 (Gpa)	1033.1	1015.3	$884.2 + 336.8x$
C12 (Gpa)	278.1	505.9	$402.6 + 163.4x$
a_c (eV)	−5.35	−3.63	$-7.5 + 5.5x$
a_v (eV)	−1.71	−3.90	$-0.8 - 6.37x$
b (eV)	−2.04	−1.50	$-2 + 0.84x$
d (eV)	−3.50	−4.16	$-4.7 - 0.1x$

[This article is copyrighted as indicated in the article. Reuse of AIP content is subject to the terms at: http://scitation.aip.org/termsconditions. Downloaded to] IP: 140.113.38.11 On: Thu, 01 May 2014 01:05:00

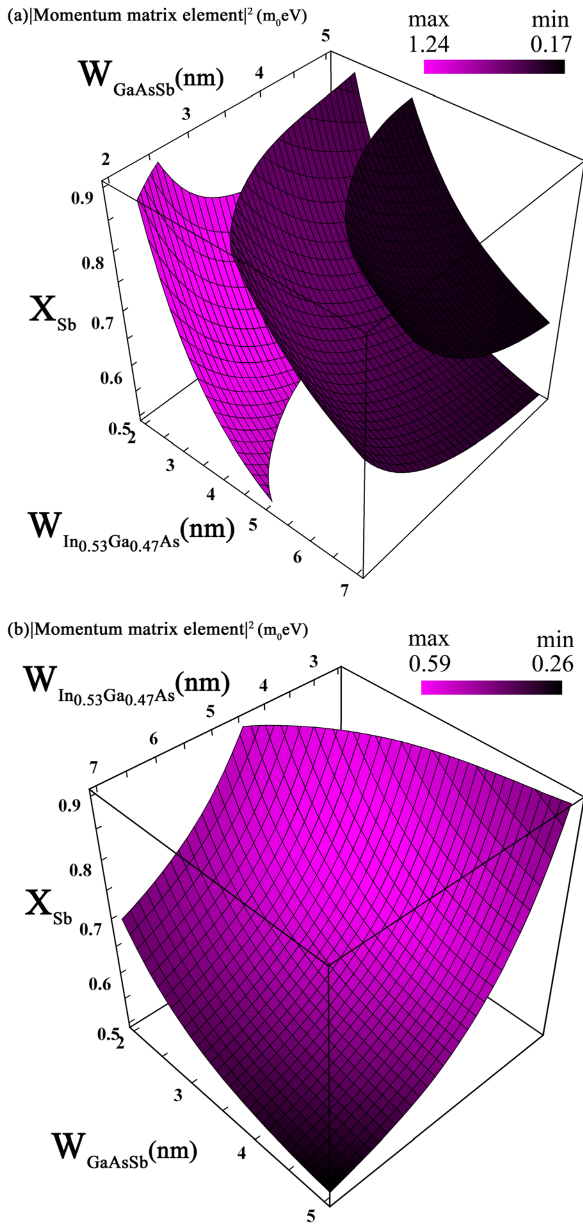

FIG. 3. (a) The 3D contour plots of corresponding squared momentum matrix elements at three wavelengths: 2, 2.5, 3 μm, and (b) only at the 2.5 μm, based on the eight band *k.p* calculations of the "W" structure with variable parameters in three axes: InGaAs width along x axis, GaAsSb width along y axis, and Sb mole fraction along z axis.

E_{hm}^{en} : electron - hole transition energy; $\hbar\omega$: photon energy; η, σ : :spin notation; n, m : conduction, valence subbands; k_t : parallel wave vector; Γ : linewidth of Lorenzian broadening; f : Fermi – Dirac distribution.

The emission wavelength of fundamental optical transition (C1 to HH1) and the corresponding squared momentum matrix element at room temperature were first calculated. Fig. 3(a) shows the 3D contour plot of the corresponding squared momentum matrix elements for the three chosen wavelengths of 2 μm, 2.5 μm, and 3 μm, where the x, y, and z axes are, in turn, values of the InGaAs layer width, GaAsSb layer width, and Sb mole fraction in GaAsSb. It is displayed in grayscale, where the brightness increases with the magnitude. The maximum and minimum values in the plot are 1.24 m_0eV and 0.17 m_0eV, respectively.

As shown in Fig. 3(a), the emission wavelength can be tuned in the range between 2 and 3 μm by varying the three parameters mentioned above. However, as the wavelength is increased, the wave function overlap decreases resulting in a smaller matrix element. A gradual increase in darkness in the plot is clearly seen as the wavelength is changed from 2 μm to 3 μm. So there is a trade-off between the long wavelength emission and the optical matrix element. It is an intrinsic feature for the "W" type QWs and the reason lies in the separately confined electrons and holes. A thicker InGaAs or GaAsSb layer leads to a smaller electron or hole quantized energy and hence a longer emission wavelength. However, it also makes the electron and hole wave functions more concentrated in the separated individual layers with less overlap. A similar trade-off exists when the Sb content in the GaAsSb layer is varied. The wavelength can be extended longer with a higher Sb content due to the reduced energy separation, δ, between the electron and the hole states. The raised conduction band edge, however, blocks the electron wave function penetration into the GaAsSb layer causing a reduction of the electron-hole wave function overlap.

As shown in Fig. 3, there are many possibilities in choosing the layer parameters to achieve the same emission wavelength. However, a different combination of the three parameters has a different strength in the transition matrix element. To show the detail of the calculated result, we plotted only the squared momentum matrix element at 2.5 μm

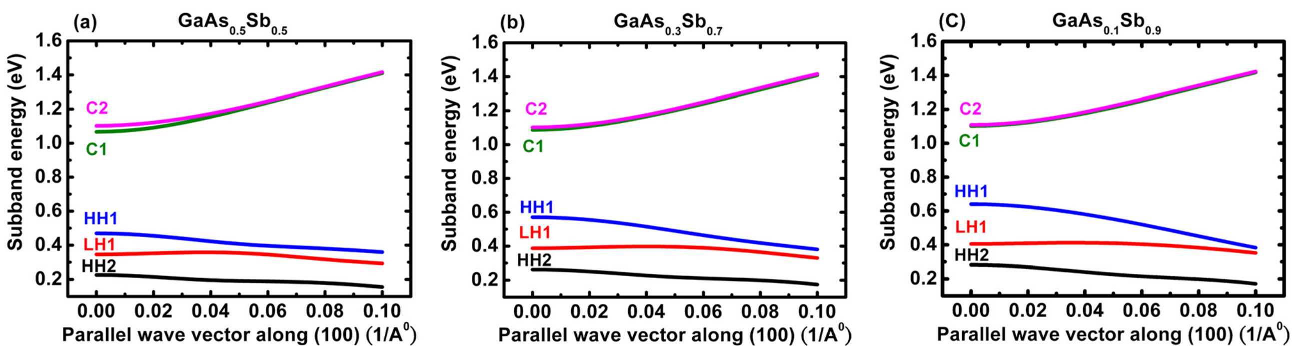

FIG. 4. The energy dispersion of the "W" QW consisting of $In_{0.53}Ga_{0.47}As/GaAs_{1-x}Sb_x/In_{0.53}Ga_{0.47}As$ (4/3/4 nm) sandwiched between $In_{0.52}Al_{0.48}As$ barrier layers for the three cases with different Sb fraction: (a) $x_{sb} = 0.5$, (b) $x_{sb} = 0.7$, and (c) $x_{sb} = 0.9$, where C1 and C2 refer to the symmetric and the anti-symmetric conduction subbands, HH1 and HH2 refer to the first and the second confined heavy hole subbands, and LH1 refers to the first confined light hole subband.

[This article is copyrighted as indicated in the article. Reuse of AIP content is subject to the terms at: http://scitation.aip.org/termsconditions. Downloaded to] IP: 140.113.38.11 On: Thu, 01 May 2014 01:05:00

TABLE II. The extracted values of the effective band gap, the energy differences of C1-C2 and HH1-LH1, and the C1 electron/HH1 hole effective masses at zone center for the three cases.

Sb fraction	0.50	0.70	0.90
Effective E_g (meV)	597.1	515.8	461.3
ΔC1–C2 (meV)	35.2	14.7	7.0
ΔHH1-LH1 (meV)	123.7	183.6	235.3
Effective m_e for C1 (m_0)	0.062	0.069	0.073
Effective m_h for HH1(m_0)	−0.105	−0.098	−0.093

wavelength in Fig. 3(b). One can see that a larger matrix element is generally obtained with a higher Sb mole fraction and thinner InGaAs/GaAsSb layers, which is also the same for other given emission wavelengths. Given such design flexibility, one has to be careful, however, when using a high Sb content in the GaAsSb layer because the material quality may degrade. We used $In_{0.52}Al_{0.48}As$ as the barrier material in our "W" structure, which has a higher conduction band offset as compared to the (Ga)InP layer used in Ref. 9 and the GaAsSb layer used in Ref. 11. Our structure has a better electron confinement and a higher energy level when the same InGaAs width is used in the structure.

Energy dispersion for three cases of "W" quantum wells was calculated. The thicknesses of InAlAs/InGaAs/$GaAs_{1-x}Sb_x$/InGaAs/InAlAs were fixed at 92/4/3/4/92 nm, but three Sb mole fractions of 0.5, 0.7, and 0.9 were used for the GaAsSb layer. The total boundary width used was 205 nm, which is large enough to ensure the wavefunction of the "W" well diminishes at the boundary. The results of the calculated E-k relation are shown in Figs. 4(a)–4(c) for the three cases. The two CB sub-bands, C1 and C2, corresponding to the symmetrical and anti-symmetrical states of the two coupled electron QWs and the HH1, LH1, and HH2 sub-bands in the VB are shown. The values of the effective band gap (C1-HH1), the energy separations of C1-C2 and HH1-LH1, the effective masses of C1 electrons, and HH1 heavy holes at the zone center are listed together in Table II for the three cases.

As seen in Table II, the effective band gap decreases from 597.1 meV to 461.3 meV as the Sb fraction increases from 0.5 to 0.9, which is caused by the raised valence band edge of the GaAsSb pseudomorphic layer. The increased valence band offset at the InGaAs/GaAsSb junction also leads to the increase of hole subband energy separation. The Δ(HH1-LH1) values increases from 123.7 to 235.3 meV. However, the conduction subband splitting Δ(C1-C2) decreases from 35.2 to 7.0 meV. The reason comes from the raised conduction band edge of GaAsSb pseudomorphic layer causing the two InGaAs electron QWs less coupled to each other. The higher the Sb fraction, the more compressively strained is within the GaAsSb layer. This shapes the energy dispersion and leads to the reduction of the HH1 effective mass from $0.105m_0$ to $0.093m_0$ as presented in Table II.

The optical transition mainly takes place between C1 and HH1, because holes are mostly populated in the HH1 band due to the large HH1-LH1 energy separation. The transition between HH1 and C2 is forbidden due to different parities in the envelop wave functions. Figs. 5(a)–5(c) show the squared matrix elements of the C1-HH1 transition for the three cases. It can be seen that the C1-HH1 transition contributes only to the TE polarization (E field parallel to the layers) near the zone center. The matrix element decreases as the in-plane wave vector moves away from the zone center. The TM component of the matrix elements rises at around the midway in the Brillouin zone where the HH1 and LH1 bands are mixed. Comparing the three cases, it is obvious that the matrix element reduces as the Sb mole fraction is increased.

Fig. 6 shows the results of TE material gain as a function of transition energy for the three cases. 2D carrier densities of 1×10^{12}, 2×10^{12}, and $3\times10^{12}\,cm^{-2}$ were used in the calculation. Fig. 7 shows the peak gain as a function of 2D carrier density. Here, we have used a line broadening factor, Γ, of 20 meV and a "W" QW thickness, Lz, of 11 nm in the calculations. As displayed in the gain spectra shown in Fig. 6, the gain increases and the spectrum broadens as more carriers are injected into the well. Except for the case with $x_{Sb}=0.9$, the peak gain of the other two ($x_{Sb}=0.5$, 0.7) can all go beyond $10^3\,cm^{-1}$ with a 2D carrier density of $3\times10^{12}\,cm^{-2}$. For InP-based type-I compressively strained InGaAs/InGaAsP QWs in near-IR 1.5 μm lasers, lower 2D carrier density values around $1.2–1.6\times10^{12}\,cm^{-2}$ are needed to get gain values over $10^3\,cm^{-1}$, which is mainly due to the better wave function overlap than "W" type QWs.[16,17] However, such optical gain and carrier density for "W" type QWs are in general sufficient to satisfy the requirements for the operation of mid-IR lasers. It should be mentioned that the calculation presented above was for only one

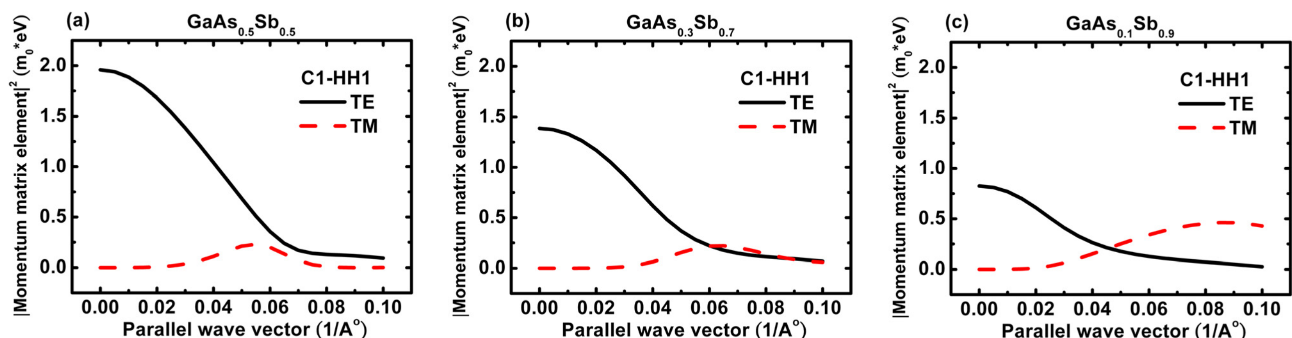

FIG. 5. The squared momentum matrix element of the C1-HH1 transition for the three cases: (a) $x_{sb}=0.5$, (b) $x_{sb}=0.7$, and (c) $x_{sb}=0.9$.

[This article is copyrighted as indicated in the article. Reuse of AIP content is subject to the terms at: http://scitation.aip.org/termsconditions. Downloaded to] IP: 140.113.38.11 On: Thu, 01 May 2014 01:05:00

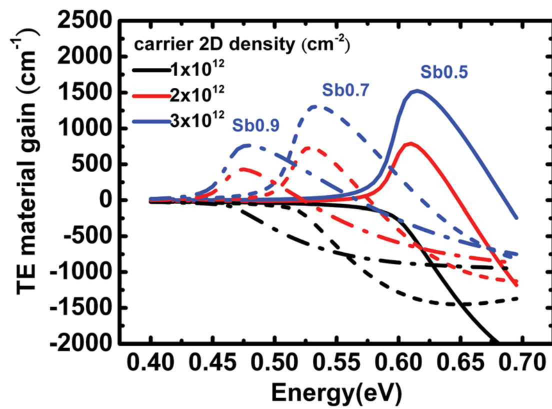

FIG. 6. The calculated TE material gain spectra for the three cases with 2D carrier densities of 1×10^{12}, 2×10^{12}, and $3 \times 10^{12}\,cm^{-2}$.

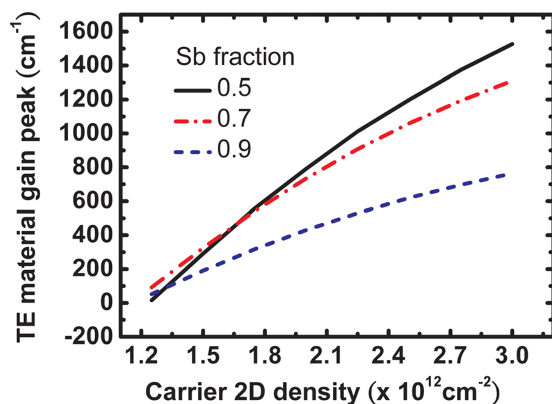

FIG. 7. The TE material gain peak value as a function of 2D carrier density for the three cases.

"W" QW. If needed (such when $x_{Sb} = 0.9$), multiple QWs can be used to boost the gain.

Looking at Figs. 7 and 5 carefully, we notice that the reduction in gain as the Sb mole fraction is increased (especially from $x_{Sb} = 0.5$ to 0.7) is not in proportion to the reduction in the magnitude of the matrix element. When the 2D carrier density is below $\sim 1.7 \times 10^{12}\,cm^{-2}$, the peak gain for the case with $x_{Sb} = 0.7$ is even superior to that of the $x_{Sb} = 0.5$ case. This is due to the reduced HH1 effective mass caused by the increased compressive strain (-1.5%) in the GaAsSb layer when a higher Sb mole fraction is used. The more balanced electron/hole effective masses cause the transparency carrier density to drop and the gain to rise. So the benefit of a more balanced electron/hole effective masses can partial compensate the gain loss caused by the reduced matrix element caused by the higher Sb content.

IV. CONCLUSIONS

We have theoretically investigated the InP based InGaAs/GaAsSb "W" type QWs for mid-IR lasers. Calculations are based on the eight band *k.p* theory and proceed by the basis expansion of the envelope function. The trade-off between the emission wavelength and the momentum matrix element is studied in the 2 μm to 3 μm range. At a given wavelength, the design with thinner InGaAs and GaAsSb layers and a higher Sb content in GaAsSb is more desirable because of a larger matrix element. Besides the emission wavelength and the matrix element, the strain in the GaAsSb layer also plays an important role in the determination of the material gain. The enhanced compressive strain in the GaAsSb layer when a high Sb content is used can reduced the transparency carrier density and increase the gain. With a proper design, the material gain of a single "W" QW is able to get above $10^3\,cm^{-1}$ with a 2D carrier density of $3 \times 10^{12}\,cm^{-2}$. The results presented in this work shows that the InP based "W" type QWs are suitable for mid-IR lasers and it provides a guideline for the design of such complex structure.

ACKNOWLEDGMENTS

We acknowledge the financial support from the National Science Council under Contract No. NSC99-2221-E-009-079-MY3, Center for Nano Science and Technology of National Chiao Tung University, National Nano Device Laboratories, and "Aim for the Top University Plan" of the National Chiao Tung University, Taiwan. The author especially would like to thank the programming help from Hong-Wen Hsieh in Professor Shun Tung Yen's lab.

[1]J. Y. T. Huang, D. R. Xu, L. J. Mawst, T. F. Kuech, I. Vurgaftman, and J. R. Meyer, IEEE J. Sel. Top. Quantum Electron. **13**, 1065 (2007).
[2]B. Chen, J. Weiyang, Y. Jinrong, A. L. Holmes, and B. M. Onat, IEEE J. Quantum Electron. **47**, 1244 (2011).
[3]C. H. Pan, C. H. Chang, and C. P. Lee, IEEE Photon. Technol. Lett. **24**, 1145 (2012).
[4]S. Sprengel, A. Andrejew, K. Vizbaras, T. Gruendl, K. Geiger, G. Boehm, C. Grasse, and M.-C. Amann, Appl. Phys. Lett. **100**, 041109 (2012).
[5]P. Werle, F. Slemr, K. Maurer, R. Kormann, R. Mücke, and B. Jänker, Opt. Lasers Eng. **37**, 101 (2002).
[6]U. Willer, M. Saraji, A. Khorsandi, P. Geiser, and W. Schade, Opt. Lasers Eng. **44**, 699 (2006).
[7]I. Vurgaftman, J. R. Meyer, N. Tansu, and L. J. Mawst, J. Appl. Phys. **96**, 4653 (2004).
[8]J. Y. Yeh, L. J. Mawst, A. A. Khandekar, T. F. Kuech, I. Vurgaftman, J. R. Meyer, and N. Tansu, Appl. Phys. Lett. **88**, 051115 (2006).
[9]J. Huang, L. Mawst, T. Kuech, X. Song, S. Babcock, C. Kim, I. Vurgaftman, J. Meyer, and A. Holmes, J. Phys. D: Appl. Phys. **42**, 025108 (2009).
[10]C. H. Pan, J. Appl. Phys. **108**, 103105 (2010).
[11]S. Sprengel, C. Grasse, K. Vizbaras, T. Gruendl, and M.-C. Amann, Appl. Phys. Lett. **99**, 221109 (2011).
[12]J. Hu, X. G. Xu, J. A. H. Stotz, S. P. Watkins, A. E. Curzon, M. L. W. Thewalt, N. Matine, and C. R. Bolognesi, Appl. Phys. Lett. **73**, 2799 (1998).
[13]I. Vurgaftman, J. Meyer, and L. Ram-Mohan, J. Appl. Phys. **89**, 5815 (2001).
[14]A. Zakharova, S. T. Yen, and K. A. Chao, Phys. Rev. B **66**, 085312 (2002).
[15]C. S. Chang and S. L. Chuang, IEEE J. Sel. Top. Quantum Electron. **1**, 218 (1995).
[16]M. Sugawara, Appl. Phys. Lett **60**, 1842 (1992).
[17]M. Sugawara and S. Yamazaki, Microwave Opt. Technol. Lett. **7**, 107 (1994).

[This article is copyrighted as indicated in the article. Reuse of AIP content is subject to the terms at: http://scitation.aip.org/termsconditions. Downloaded to] IP: 140.113.38.11 On: Thu, 01 May 2014 01:05:00